

Full Length Research Paper

RMS and power measurement using the dual-tree complex wavelet transform

Fahri Vatansever

Department of Electronic and Computer Education, Faculty of Technical Education, Sakarya University, Esentepe Campus, 54187-Sakarya/Turkey. E-mail: fahriv@sakarya.edu.tr. Tel: 90.264.2956463. Fax: 90.264.2956424.

Accepted 23 August, 2010

Measurement of signal's effective values and calculation of active-reactive-apparent-distortion powers using these measured effective values are one of the most important tasks in the energy systems. Calculations of the effective values and powers by using the classical methods are based on the Fourier transformations. On the other hand, due to the Fourier transformation having some disadvantages such as it's being used in constant windowing functions and complex mathematical operations; it causes some undesired cases in the analysis of abrupt changed dynamic signals. Whereas, they are some alternative approaches based on the discrete wavelet transform and discrete wavelet packet transform. However, in the case of using the real wavelets, some problems occur such as oscillations, shift variance and aliasing. In this work, dual-tree complex wavelet transform has been used to calculate the effective values of the current, voltage signals and the power parameters. It has been observed that the carried out simulation and experiment's results and the real values are consistent. Also, it has been shown in the simulations that the method is almost unaffected from the signal shifting.

Key words: RMS, power, dual-tree complex wavelet transform.

INTRODUCTION

One of the important task in the power systems is measuring or calculating the current, voltage signal's effective (root-mean-square) (RMS) values in total or separately using its harmonics and this task continuous to calculate the power parameters (active-reactive-apparent-distortion power and power factor) by using the measured effective voltage, current values. Classical ways to analyze the harmonics and power are based on the Fourier Transformation (FT). Harmonic distribution of the signals can be calculated by taking their Fourier transformations and then from here, their RMS and power values can be calculated. On the other hand, Fourier transformations fail to detect sudden changes, which may occur in the signals because they use fixed windowing functions and thus error rates of the measurement increase in the case of these situations. In addition, complex mathematical operations (trigonometric, exponential) need to be done in the Fourier based approximations. However in recent years, wavelet transformations are also heavily used in the power analysis. Calculation of RMS values of the signals

and the active power using the discrete wavelet transformation (DWT) can be found in Ref. (Yoon and Devaney, 1998). Also, calculation of the reactive power using DWT and designed appropriate 90° phase-shift networks was carried out in Ref. (Yoon and Devaney, 2000). Calculation of RMS and active power value of each harmonic and total RMS and active power value using the discrete wavelet packet transform (DWPT) are located in (Hamid et al., 2002). Also, calculation of the fundamental harmonic power values can be found in (Vatansever and Ozdemir, 2010). Calculation of the RMS and phase angle values of the signal's fundamental harmonic using the DWPT and the Hilbert transform and obtaining the fundamental harmonic powers from here are given in (Vatansever and Ozdemir, 2009a). Again, calculation of the fundamental harmonic and total power parameters using the DWPT and the Hilbert transform are given in (Vatansever and Ozdemir, 2009b). RMS value calculations in WT domain can be found in (Zhu, 2004). RMS and power approaches in the frequency-time-wavelet domains are summarized comparatively in

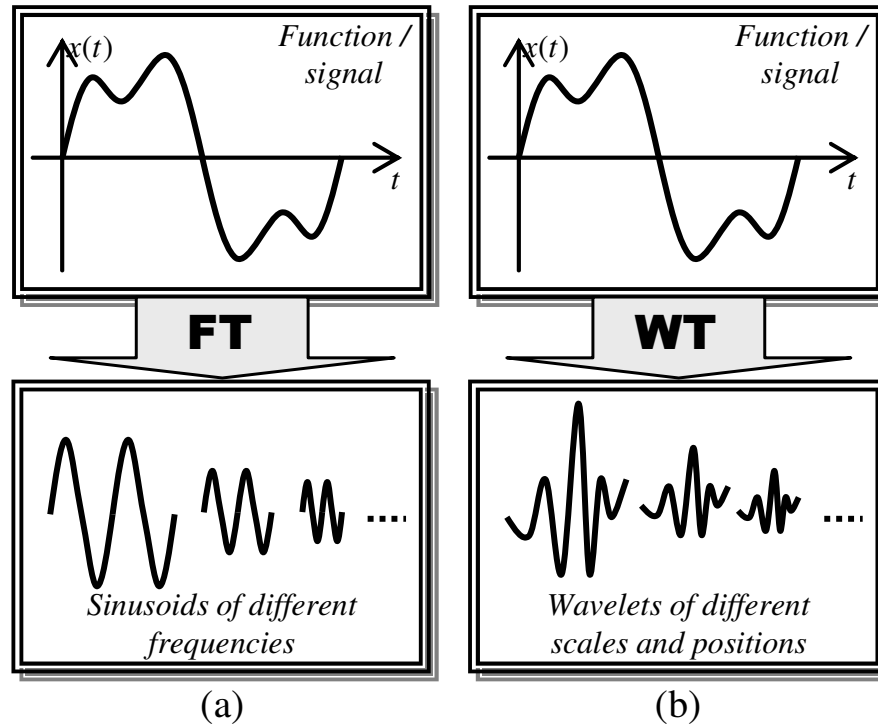


Figure 1. Graphically (a) Fourier (b) Wavelet process.

(Morsi and El-Hawary, 2009).

In this work unlike the above studies, RMS value and active-reactive-apparent-distortion power and power factor calculations were performed using the dual-tree complex wavelet transform (DT CWT). For this purpose, validity of the proposed equations is shown with the performed simulation and experimental measurement results. It is known that the DT CWT is less affected from the signal shifting and this is the one of the most important advantages of the DT CWT. In this work, this advantage is also shown in simulations to calculate the RMS values.

This paper is organized as follows: Wavelet transforms (DWT, DWPT and DT CWT) is briefly and comparatively explained in the "Materials" section. Details of presented methods for RMS calculation and its simulations results are given in the "Methods" section. Also details of presented methods for power calculation and its simulations and experimental results are given in the "Results" section.

MATERIALS AND METHODS

Materials

The dual-tree complex wavelet transforms

If any of the $x(t)$ signal's Fourier transform is taken then, its frequency domain components can be obtained. That is to say,

$x(t)$ can be expressed as a sum of the sinusoids (trigonometric functions), which have different amplitudes and frequencies. Mathematically, $X(\omega)$, which is the Fourier transform of $x(t)$, is given as

$$X(\omega) = F\{x(t)\} = \int_{-\infty}^{\infty} x(t) \cdot e^{-j\omega t} dt \quad (1)$$

In here, $x(t)$ signal is first multiplied by complex multiplier in the whole time range and then summed (Debnath, 2002; Goswami and Chan, 1999; Mathworks, 2000). As a result, transformation gives $X(\omega)$ Fourier coefficients. Thus, the function/signal can be expressed as:

$$x(t) = a_0 + a_1 \cos(\omega t + \theta_1) + a_2 \cos(2\omega t + \theta_2) + \dots = \sum_{k=0}^{\infty} a_k \cos(k\omega t + \theta_k) \quad (2)$$

This is summarized graphically in Figure 1a (Debnath, 2002; Goswami and Chan, 1999; Mathworks, 2000).

Similarly, CWT of $x(t)$ is defined mathematically as

$$W(a, b) = \frac{1}{\sqrt{a}} \int_{-\infty}^{\infty} x(t) \cdot \overline{\psi\left(\frac{t-b}{a}\right)} dt \quad (3)$$

Where, a is scaling/dilation parameter, b is translation/shift

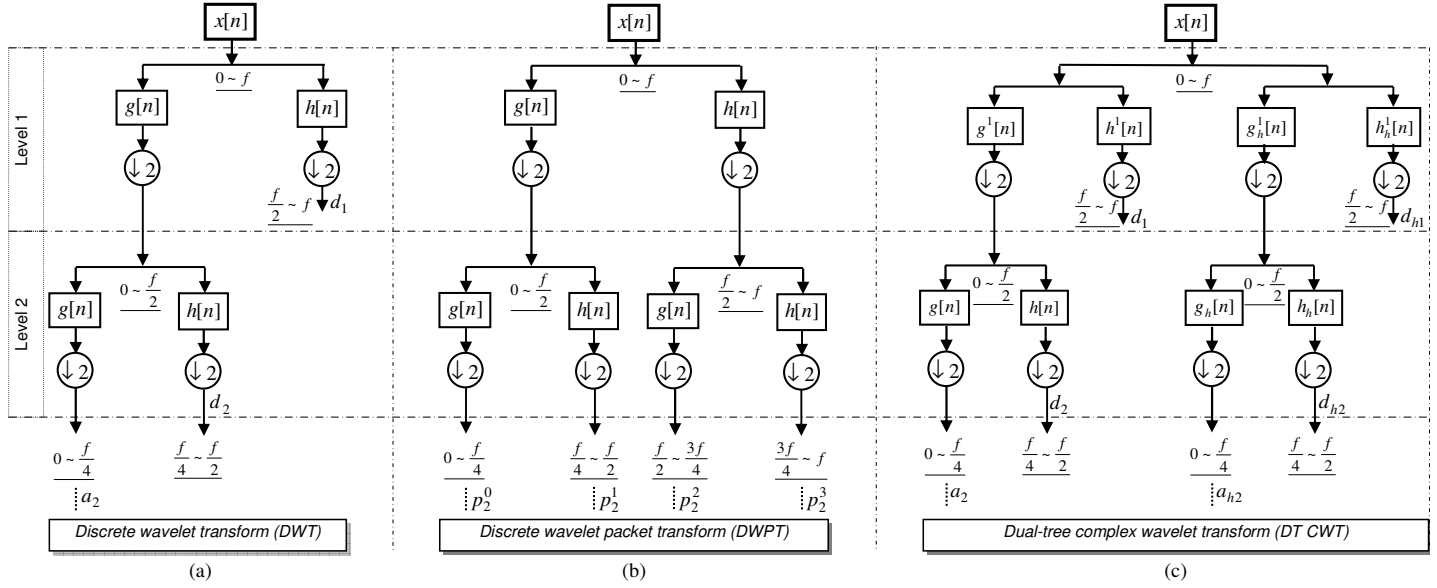


Figure 2. 2-level DWT, DWPT and DT CWT decomposition trees.

parameter, $x(t)$ is signal, ψ is wavelet function, $W(a, b)$ is the continuous wavelet transformation of the signal and $a > 0, b \in \mathfrak{R}$ in the equation (Debnath, 2002; Goswami and Chan, 1999; Mathworks, 2000). As can be seen from here, CWT is defined as the sum of the multiplied of $x(t)$ signal with the scaled and shifted version of the ψ wavelet function in the whole time range.

$$W(scale, position) = \int_{-\infty}^{+\infty} x(t) \cdot \psi(scale, position, t) dt \quad (4)$$

As a result of CWT, many W wavelet coefficients are obtained appropriate to the scale and location of the function. Each coefficient multiplied with the appropriately scaled and shifted wavelet forms the wavelet components of the original function/signal. Thus, analyzed $x(t)$ function/signal can be expressed as

$$x(t) = W_0 \cdot \phi(t) + W_1 \cdot \psi(t) + \sum_{p,q} W_{p,q} \cdot \psi(2^p t - q) \quad (5)$$

This is summarized graphically in Figure 1b (Debnath, 2002; Goswami and Chan, 1999; Mathworks, 2000).

Mathematically, DWT of the $x(t)$ signal is given as,

$$\left. \begin{matrix} a = \frac{1}{2^j} \\ b = \frac{k}{2^j} \end{matrix} \right\} \Rightarrow w_{j,k} = W_{\psi} x \left(\frac{k}{2^j}, \frac{1}{2^j} \right) = \sqrt{2^j} \int_{-\infty}^{\infty} x(t) \psi \left(\frac{t - k/2^j}{1/2^j} \right) dt \quad (6)$$

Where $j, k \in \mathbb{Z}$ (Debnath, 2002; Goswami and Chan, 1999). In the discrete wavelet transformation, which has one-sided decomposition tree (Figure 2a), discrete signal is applied to the filters, where $g[n]$ and $h[n]$ low pass and high pass filters respectively, and then obtained data are down sampling by 2. So that, while approximations of the signal emerge in the low pass filters branch, details of the signal emerge in the high pass filter branch. In the next decomposition level, previously obtained approximations of the signal are again applied to the low and high pass filters. Then obtained data are down sampling by 2, so that the sequential process continuous in this manner. In the wavelet packet transform, which is the next advanced stage of the DWT, there is a dual-sided decomposition tree (Figure 2b) (Debnath, 2002; Goswami and Chan, 1999; Mathworks, 2000).

In case of using real wavelets, four major problems arise. These are:

- Oscillations
- Shift variance
- Aliasing
- Lack of directionality (Kingsbury, 1998; Selesnick et al., 2005).

Whereas, dual-tree complex wavelet transform has following properties (Kingsbury, 1998; Selesnick et al., 2005).

- Approximate shift invariance
- Good directional selectivity in 2-dimensions
- Perfect reconstruction using short linear phase filters
- Limited redundancy
- Efficient order-N computation

In the DT CWT, in addition to one-sided decomposition tree in the DWT, there is another parallel decomposition tree, which has filter set composed of the Hilbert transform of the filters in this tree (Figure 2c). So that, while the real component coefficients of the signal are obtained from a tree, imaginary component coefficients are obtained from the other tree.

Methods

RMS value calculation

The effective/RMS value of any $v(t)$ signal is given as (IEEE Working Group on Nonsinusoidal Situations, 1996):

$$V_{RMS} = \sqrt{\frac{1}{T} \int_T v^2(t) dt} \tag{7}$$

RMS value of a $v(t)$ voltage/current signal, which has DC component with harmonics, can be calculated as,

$$v(t) = V_{DC} + V_{m1} \cdot \text{Cos}(\omega t) + V_{m2} \cdot \text{Cos}(2\omega t) + V_{m3} \cdot \text{Cos}(3\omega t) + \dots \tag{8}$$

$$V_{RMS} = \sqrt{V_{DC}^2 + \left(\frac{V_{m1}}{\sqrt{2}}\right)^2 + \left(\frac{V_{m2}}{\sqrt{2}}\right)^2 + \left(\frac{V_{m3}}{\sqrt{2}}\right)^2 + \dots}$$

$$v(t) = V_{DC} + V_1 \cdot \text{Cos}(\omega t) + V_2 \cdot \text{Cos}(2\omega t) + V_3 \cdot \text{Cos}(3\omega t) + \dots \tag{9}$$

$$V_{RMS} = \sqrt{V_{DC}^2 + V_1^2 + V_2^2 + V_3^2 + \dots}$$

In the Equations 8 to 9, V_{m1} shows the maximum value of the first/fundamental harmonic, on the other hand, V_1 shows the effective value of the first/fundamental harmonic.

Calculation of the RMS using DWT can be found in (Yoon and Devaney, 1998). If a $v(t)$ signal, which has T period, is applied to discrete wavelet transform till j_0 level, then the RMS value is given as (Yoon and Devaney, 1998);

$$V_{RMS} = \sqrt{\frac{1}{T} \int_0^T v^2(t) dt} = \sqrt{\frac{1}{T} \sum_k c_{j_0,k}^2 + \frac{1}{T} \sum_{j \geq j_0} \sum_k d_{j,k}^2} = \sqrt{V_{j_0}^2 + \sum_{j \geq j_0} V_j^2} \tag{10}$$

In Equation 10, c is scaling (approximation) coefficient and d is wavelet (detail) coefficient. If the Equation 10 is rearranged for the DT CWT, two alternative ways emerge. These are as follow;

a) Using the one-side of the decomposition tree: If a discrete $v[n]$ signal, which has N values such as Equation 8, is applied to the DT CWT decomposition till level s ,

$$V_a = \sqrt{\frac{1}{N} \sum_{k=1}^{N/2^s} a_s^2[k]} \tag{11}$$

$$V_d = \sqrt{\sum_{m=1}^s \left\{ \frac{1}{N} \sum_{k=1}^{N/2^s} d_m^2[k] \right\}} \Rightarrow V_{RMS} = \sqrt{2(V_a^2 + V_b^2)}$$

Or RMS value can be calculated using following equations.

$$V_{h,a} = \sqrt{\frac{1}{N} \sum_{k=1}^{N/2^s} a_{h,s}^2[k]} \tag{12}$$

$$V_{h,d} = \sqrt{\sum_{m=1}^s \left\{ \frac{1}{N} \sum_{k=1}^{N/2^s} d_{h,m}^2[k] \right\}} \Rightarrow V_{RMS} = \sqrt{2(V_{h,a}^2 + V_{h,b}^2)}$$

b) Using the both-sides of the decomposition tree: If a discrete $v[n]$ signal, which has N values such as Eq.8, is applied to the DT CWT decomposition till level s , RMS value can be calculated using following Equations.

$$V_{c,a} = \sqrt{\frac{1}{N} \sum_{k=1}^{N/2^s} |a_s[k] + ja_{h,s}[k]|^2} \tag{13}$$

$$V_{c,d} = \sqrt{\sum_{m=1}^s \left\{ \frac{1}{N} \sum_{k=1}^{N/2^s} |d_m[k] + jd_{h,m}[k]|^2 \right\}} \Rightarrow V_{RMS} = \sqrt{V_{c,a}^2 + V_{c,d}^2}$$

In Equations. 11 to 13, a_s shows the real part of approximation coefficient at level s ; d_m , real part of details coefficient at level m ; $a_{h,s}$, imaginary part of approximation coefficient at level s and $d_{h,m}$ shows the imaginary part of details coefficient at level m .

Simulations for RMS calculations

To perform the simulations of the RMS calculations, a user interface program has been designed in the MATLAB (Mathworks, 2000; <http://taco.poly.edu/WaveletSoftware/>). This program performs the RMS calculation using the Equations 11 - 13. First of all, data are loaded to the program from the peripheral devices, their graphics are being drawn and then the RMS values are calculated. As a first simulation, following signal is decomposed in DT CWT taking 512 samples from its one period till level 5, where $\omega = 2\pi 50$.

$$v(t) = \sqrt{2} \left\{ 220.0 \text{Cos}(\omega t) + 50.0 \text{Cos}(3\omega t) - 10.0 \text{Cos}(5\omega t) + 2.0 \text{Cos}(7\omega t) - 0.4 \text{Cos}(9\omega t) \right\} \tag{14}$$

Resulted simulation screen is given in Figure 3. Similarly, some simulation's results, expressions, obtained RMS values using real and DT CWT and relative errors are given in Table 1. Their screenshots are also given in Figure 4. The simulations are carried out in the Table 1 by using the signals, which are given in Ref. (Yoon and Devaney, 1998) for row 3, Ref. (Zhu, 2004) for row 4 and Ref. (Hamid, Mardiana, Kawasaki, 2002) for row 5. As shown from the Table 1 that, real values and the values, which are obtained using DT CWT are consistent.

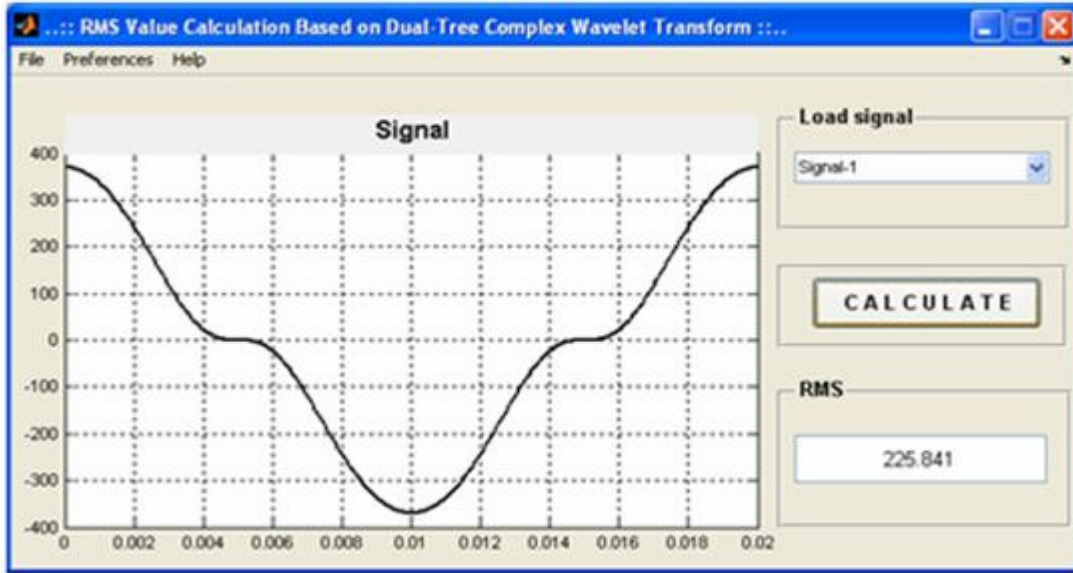


Figure 3. Screenshot of the first simulation.

Table 1. Simulation results.

f (Hz)	Signal	True RMS	DT CWT RMS	Relative error (%)
50	$\sqrt{2} \left\{ \begin{array}{l} 220.0\text{Cos}(\omega t) + 50.0\text{Cos}(3\omega t) - \\ 10.0\text{Cos}(5\omega t) + 2.0\text{Cos}(7\omega t) - \\ 0.4\text{Cos}(9\omega t) \end{array} \right\}$	225.841006019722	225.841010614455	0.000002034499
60	$\sqrt{2} \left\{ \begin{array}{l} 220.0\text{Cos}(\omega t - 10^\circ) + 40.0\text{Cos}(5\omega t + 25^\circ) \\ + 12.0\text{Cos}(7\omega t) - 4.0\text{Cos}(13\omega t + 30^\circ) + \\ 1.0\text{Cos}(17\omega t - 40^\circ) + 0.04\text{Cos}(23\omega t) \end{array} \right\}$	223.966518926379	223.966523472953	0.000002030024
60	$\sqrt{2}\text{Sin}(\omega t) + \sqrt{2}\text{Sin}(5\omega t + 150^\circ) + \sqrt{2}\text{Sin}(11\omega t)$	1.732050807569	1.732050829498	0.000001266062
50	$100 + 66.7\text{Cos}(2\omega t) - 13.3\text{Cos}(4\omega t) + 5.7\text{Cos}(6\omega t) - 3.1\text{Cos}(8\omega t) + 2.0\text{Cos}(10\omega t)$	111.067276909088	111.067279228007	0.000002087851
60	$\sqrt{2} \left\{ \begin{array}{l} 1.0\text{Sin}(\omega t) + 0.2\text{Sin}(3\omega t + 135^\circ) + \\ 0.2\text{Sin}(5\omega t + 150^\circ) + 0.1\text{Sin}(7\omega t + 140^\circ) \\ + 0.08\text{Sin}(9\omega t + 40^\circ) + \\ 0.1\text{Sin}(11\omega t + 15^\circ) + 0.1\text{Sin}(13\omega t + 150^\circ) \end{array} \right\}$	1.056598315349	1.056598336156	0.000001969189

One of the biggest encountered problems in case of using real wavelets is negative affection from the signal shifting. However, DT CWT transformation is nearly independent from the shifting. This case is given in Table 2 comparatively for the sample signal, which

is given in the first row of the Table 1, by shifting it 0, 0.005, 0.01, 0.015 and 0.02 s, respectively. As seen from the Table 2 that calculations of the RMS values using the DT CWT are not affected from the signal shifting.

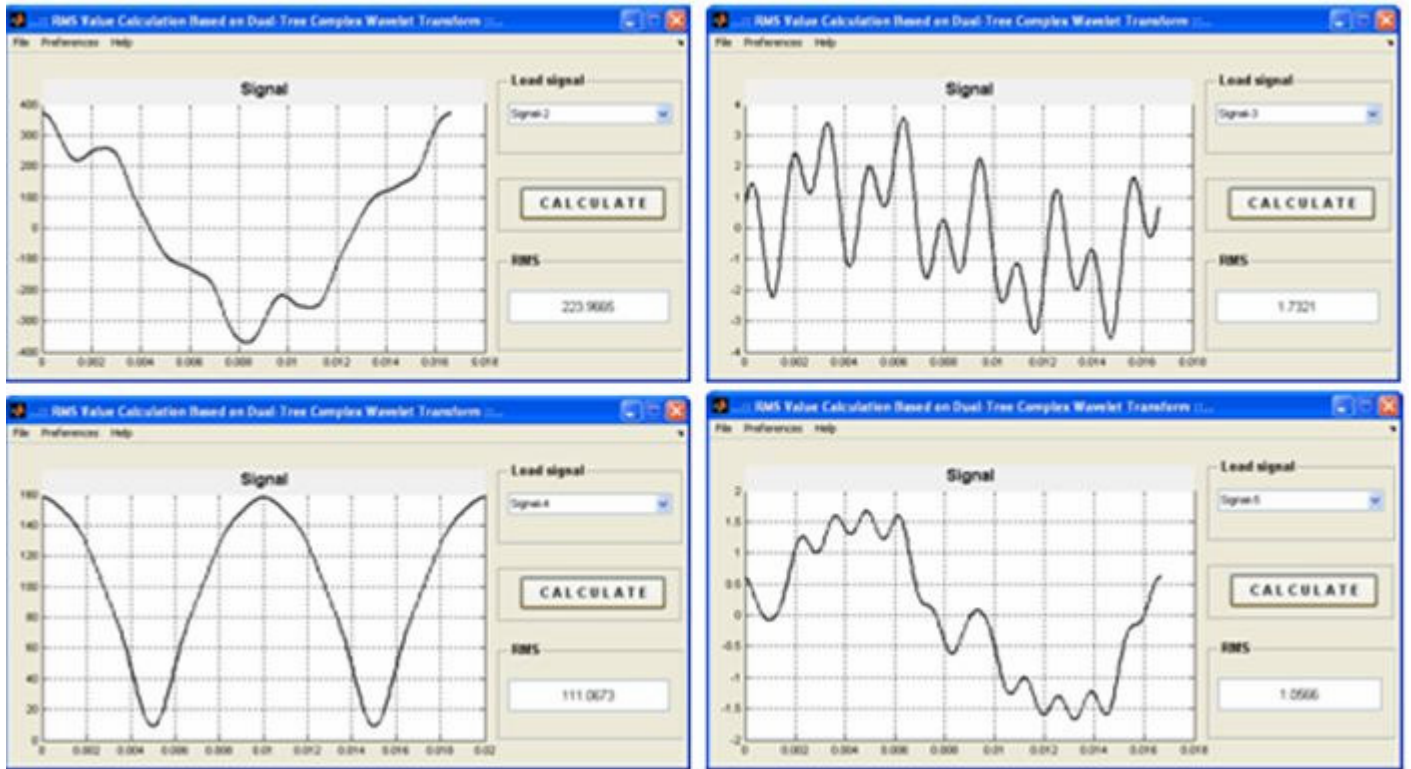


Figure 4. Simulation screenshots.

Table 2. Signal shifting and RMS values.

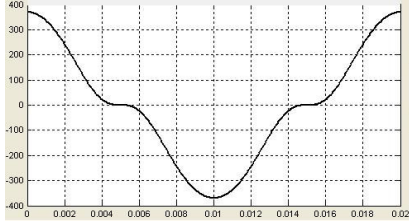
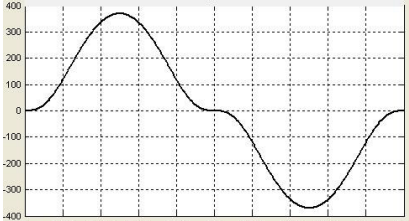
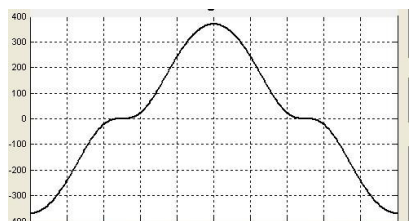
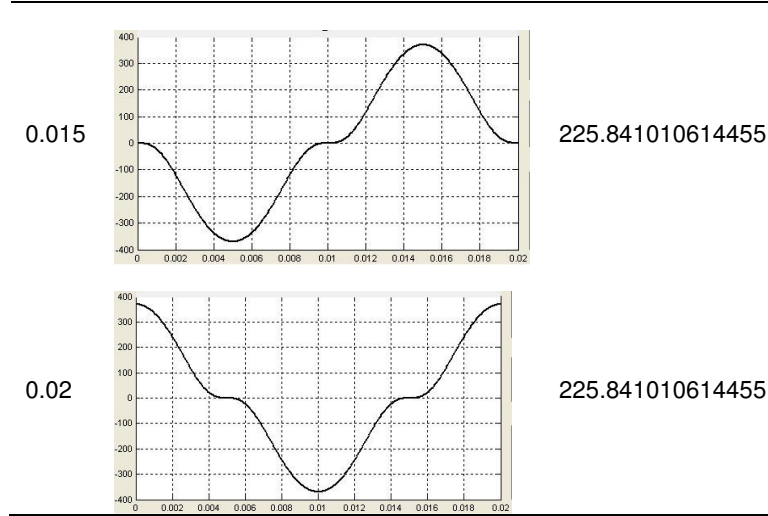
Shifting (s)	Signal	RMS value
0.000		225.841010614455
0.005		225.841010614455
0.01		225.841010614455

Table 2. Contd.



Power calculation

In the monophas power system;

▪ Apparent power: $S = V_{RMS} \cdot I_{RMS}$ (15)

▪ Active power: $P = \frac{1}{T} \int_0^T v(t) \cdot i(t) \cdot dt$ (16)

▪ Reactive power: $Q = \frac{1}{T} \int_0^T v_{t-90^\circ}(t) \cdot i(t) \cdot dt$ (17)

▪ Distortion power: $D = \sqrt{S^2 - (P^2 + Q^2)}$ (18)

▪ Power factor: $\text{Cos}(\varphi) = \frac{P}{S}$ (19)

Are given, where $v(t)$ and $i(t)$ are voltage and current signals respectively (Morsi and El-Hawary, 2009; IEEE Working Group on Nonsinusoidal Situations, 1996).

Calculation of the DT CWT based RMS values can be found in Equation 11 to 13. Here two alternative ways to calculate apparent power are emerging. If discrete $v[n]$ and $i[n]$ voltage and current signals, which have N values such as in Equation 8, are applied to the DT CWT decomposition till level s , apparent power can be calculated using the following equations.

a) Using the one-side of the decomposition tree:

$$S = V_{RMS} \cdot I_{RMS} = 2\sqrt{(V_a^2 + V_b^2)(I_a^2 + I_b^2)} \quad (20)$$

Or

$$S = V_{RMS} \cdot I_{RMS} = 2\sqrt{(V_{h,a}^2 + V_{h,b}^2)(I_{h,a}^2 + I_{h,b}^2)} \quad (21)$$

b) Using the both-sides of the decomposition tree:

$$S = V_{RMS} \cdot I_{RMS} = \sqrt{(V_{c,a}^2 + V_{c,d}^2)(I_{c,a}^2 + I_{c,d}^2)} \quad (22)$$

Calculation of the active power using the DWT is given in Ref. (Yoon and Devaney, 1998). If $v(t)$ and $i(t)$ voltage and current signals, which have T periods, are multiplied and then applied to discrete wavelet transform till j_0 level, then the power value is given as (Yoon and Devaney, 1998),

$$P = \frac{1}{T} \int_0^T v(t) \cdot i(t) \cdot dt = \frac{1}{T} \sum_k c_{j_0,k}^v \cdot c_{j_0,k}^i + \frac{1}{T} \sum_{j \geq j_0} \sum_k d_{j,k}^v \cdot d_{j,k}^i = P_{j_0} + \sum_{j \geq j_0} P_j \quad (23)$$

In Equation 23, c^v and c^i are scaling (approximation) coefficients, d^v and d^i are wavelet (detail) coefficients of voltage and current, respectively. If the Eq. 23 is rearranged for the DT CWT, two alternative ways emerge. If discrete $v[n]$ and $i[n]$ voltage and current signals, which have N values such as in Eq.8, are applied to the DT CWT decomposition till level s , active power can be calculated using the following equations.

a) Using the one-side of the decomposition tree:

$$P = 2 \left\{ \frac{1}{N} \sum_{k=1}^{N/2^s} a_s^v[k] \cdot a_s^i[k] + \sum_{m=1}^s \left\{ \frac{1}{N} \sum_{k=1}^{N/2^s} d_m^v[k] \cdot d_m^i[k] \right\} \right\} \quad (24)$$

Or

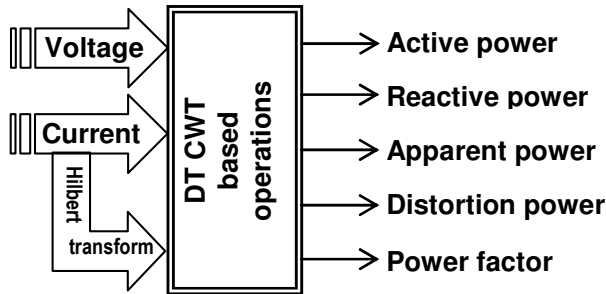


Figure 5. Block diagram of calculation/measurement method.

$$P = 2 \left\{ \frac{1}{N} \sum_{k=1}^{N/2^s} a_{h,s}^v[k] a_{h,s}^i[k] + \sum_{m=1}^s \left\{ \frac{1}{N} \sum_{k=1}^{N/2^s} d_{h,m}^v[k] d_{h,m}^i[k] \right\} \right\} \quad (25)$$

b) Using the both-sides of the decomposition tree:

$$P = 2 \left\{ \frac{1}{N} \sum_{k=1}^{N/2^s} \text{Re}\{a_s^v[k] + ja_{h,s}^v[k]\} \text{Re}\{a_s^i[k] + ja_{h,s}^i[k]\} + \sum_{m=1}^s \left\{ \frac{1}{N} \sum_{k=1}^{N/2^s} \text{Re}\{d_m^v[k] + jd_{h,m}^v[k]\} \text{Re}\{d_m^i[k] + jd_{h,m}^i[k]\} \right\} \right\} \quad (26)$$

Or

$$P = 2 \left\{ \frac{1}{N} \sum_{k=1}^{N/2^s} \text{Im}\{a_s^v[k] + ja_{h,s}^v[k]\} \text{Im}\{a_s^i[k] + ja_{h,s}^i[k]\} + \sum_{m=1}^s \left\{ \frac{1}{N} \sum_{k=1}^{N/2^s} \text{Im}\{d_m^v[k] + jd_{h,m}^v[k]\} \text{Im}\{d_m^i[k] + jd_{h,m}^i[k]\} \right\} \right\} \quad (27)$$

In Eqns. 24-27, a_s^v and a_s^i are real part of approximation coefficient at level s of voltage and current, respectively. d_m^v and d_m^i are real part of details coefficient at level m of voltage and current, respectively. Similarly $a_{h,s}^v$, $a_{h,s}^i$, $d_{h,m}^v$ and $d_{h,m}^i$ are imaginary part of approximation and details coefficient at level s of voltage and current, respectively.

Similarly, if discrete $v[n]$ and $i[n]$ voltage and current signals, which have N values such as in Eq.8, are applied to the DT CWT decomposition till level s , two alternative ways to calculate the DT CWT based reactive power emerge. These are as follows;

a) Using the one-side of the decomposition tree:

$$Q = -2 \left\{ \frac{1}{N} \sum_{k=1}^{N/2^s} a_s^v[k] a_s^{\text{Im}(\mathcal{H}\{i\})}[k] + \sum_{m=1}^s \left\{ \frac{1}{N} \sum_{k=1}^{N/2^s} d_m^v[k] d_m^{\text{Im}(\mathcal{H}\{i\})}[k] \right\} \right\} \quad (28)$$

or

$$Q = -2 \left\{ \frac{1}{N} \sum_{k=1}^{N/2^s} a_{h,s}^v[k] a_{h,s}^{\text{Im}(\mathcal{H}\{i\})}[k] + \sum_{m=1}^s \left\{ \frac{1}{N} \sum_{k=1}^{N/2^s} d_{h,m}^v[k] d_{h,m}^{\text{Im}(\mathcal{H}\{i\})}[k] \right\} \right\} \quad (29)$$

b) Using the both-sides of the decomposition tree:

$$Q = -2 \left\{ \frac{1}{N} \sum_{k=1}^{N/2^s} \text{Re}\{a_s^v[k] + ja_{h,s}^v[k]\} \text{Re}\{a_s^{\text{Im}(\mathcal{H}\{i\})}[k] + ja_{h,s}^{\text{Im}(\mathcal{H}\{i\})}[k]\} + \sum_{m=1}^s \left\{ \frac{1}{N} \sum_{k=1}^{N/2^s} \text{Re}\{d_m^v[k] + jd_{h,m}^v[k]\} \text{Re}\{d_m^{\text{Im}(\mathcal{H}\{i\})}[k] + jd_{h,m}^{\text{Im}(\mathcal{H}\{i\})}[k]\} \right\} \right\} \quad (30)$$

or

$$Q = -2 \left\{ \frac{1}{N} \sum_{k=1}^{N/2^s} \text{Im}\{a_s^v[k] + ja_{h,s}^v[k]\} \text{Im}\{a_s^{\text{Im}(\mathcal{H}\{i\})}[k] + ja_{h,s}^{\text{Im}(\mathcal{H}\{i\})}[k]\} + \sum_{m=1}^s \left\{ \frac{1}{N} \sum_{k=1}^{N/2^s} \text{Im}\{d_m^v[k] + jd_{h,m}^v[k]\} \text{Im}\{d_m^{\text{Im}(\mathcal{H}\{i\})}[k] + jd_{h,m}^{\text{Im}(\mathcal{H}\{i\})}[k]\} \right\} \right\} \quad (31)$$

In Equations 28 to 31, $a_s^{\text{Im}(\mathcal{H}\{i\})}$, $a_{h,s}^{\text{Im}(\mathcal{H}\{i\})}$, $d_m^{\text{Im}(\mathcal{H}\{i\})}$ and $d_{h,m}^{\text{Im}(\mathcal{H}\{i\})}$ are real and imaginary part of approximation and details coefficient at level s of imaginary part of Hilbert transform of current, respectively.

Distortion power and power factor values can be calculated using the above Equation 20 to 22, Equation 24 to 27 and Equation 28 to 31 at the Equation 18 and 19. DT CWT based power calculations procedure is summarized in Figure 5.

RESULTS

To perform the simulations of the power calculations, a user interface program has been also designed in the MATLAB as was in the calculation of the RMS values (Mathworks, 2000; <http://taco.poly.edu/WaveletSoftware/>). As a first simulation, following voltage and current signals (Equation 32), which are also given in (Yoon and Devaney, 1998), are decomposed in DT CWT taking 512 samples from its one period till level 5, where $\omega = 2\pi 60$.

$$\left. \begin{aligned} v(t) &= \sqrt{2} \sin(\omega t) + \sqrt{2} \sin(5\omega t + 150^\circ) + \sqrt{2} \sin(11\omega t) \\ i(t) &= \sqrt{2} \sin(\omega t + 60^\circ) + \sqrt{2} \sin(5\omega t) + \sqrt{2} \sin(11\omega t) \end{aligned} \right\} \quad (32)$$

Resulted simulation's screen shoot is given in Figure 6 and the comparative results are given in Table 4.

As a second simulation, following voltage and current signals, which are also given in Ref. (Yoon and Devaney, 2000) (Equation 33), are decomposed in DT CWT taking 512 samples from its one period till level 5, where $\omega = 2\pi 60$.

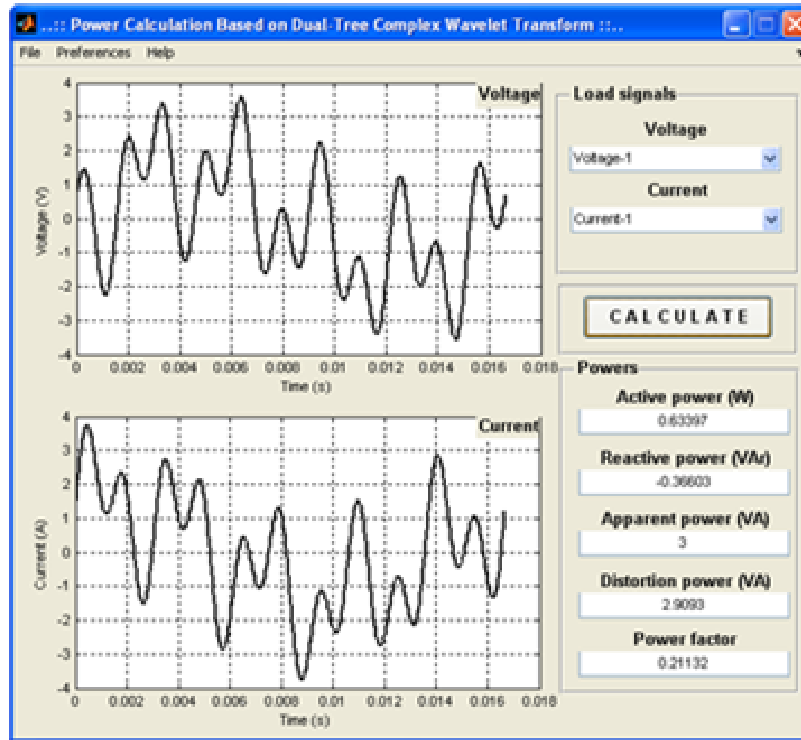


Figure 6. Screenshot for first simulation.

Table 3. Comparative result for first simulation.

	True	Ref. (Yoon and Devaney, 1998)	DT CWT
Active power (W)	0.6340	0.634	0.633974609129
Reactive power (VAr)	-0.3660	-	-0.366025428148
Apparent power (VA)	3.0000	-	3.000000075964
Distortion power (VA)	2.9093	-	2.909312983629
Power factor	0.2113	-	0.211324864359

Table 4. Comparative results for second simulation.

	True	Ref. (Yoon and Devaney, 2000)	Ref. (Vatansever and Ozdemir, 2009b)	DT CWT
Active power (W)	1.3411	1.341	1.341	1.341081392841
Reactive power (VAr)	0.9269	0.927	0.926	0.926867802764
Apparent power (VA)	6.0000	6.000	6.000	6.000000094158
Distortion power (VA)	5.7743	5.774	5.774	5.774289385186
Power factor	0.2235	-	0.223	0.223513561965

$$\begin{aligned}
 v(t) &= \sqrt{2} \left\{ \begin{aligned} &1.0\sin(\omega t) + 1.0\sin(5\omega t + 150^\circ) + 1.0\sin(11\omega t) + 1.0\sin(13\omega t + 90^\circ) + \\ &1.0\sin(23\omega t - 45^\circ) + 1.0\sin(45\omega t + 45^\circ) \end{aligned} \right\} \\
 i(t) &= \sqrt{2} \left\{ \begin{aligned} &1.0\sin(\omega t + 60^\circ) + 1.0\sin(5\omega t) + 1.0\sin(11\omega t) + 1.0\sin(13\omega t) + \\ &1.0\sin(23\omega t) + 1.0\sin(45\omega t - 45^\circ) \end{aligned} \right\}
 \end{aligned}
 \tag{33}$$

Resulted simulation's screen shoot is given in Figure 7 and the comparative results are given in Table 3.

As seen from the performed simulations (Tables 3 - 4),

real results and the results, which are obtained using the DT CWT based power calculation/measurements, are consistent.

A three phase balanced power system's experimental setup was realized to analyze the practical results (Figure 8a). Here, DT CWT based power calculations are performed by reading the voltage and current values of each phase (Figure 8b). As was in the simulations, experimental measurement results and the calculation results are also consistent.

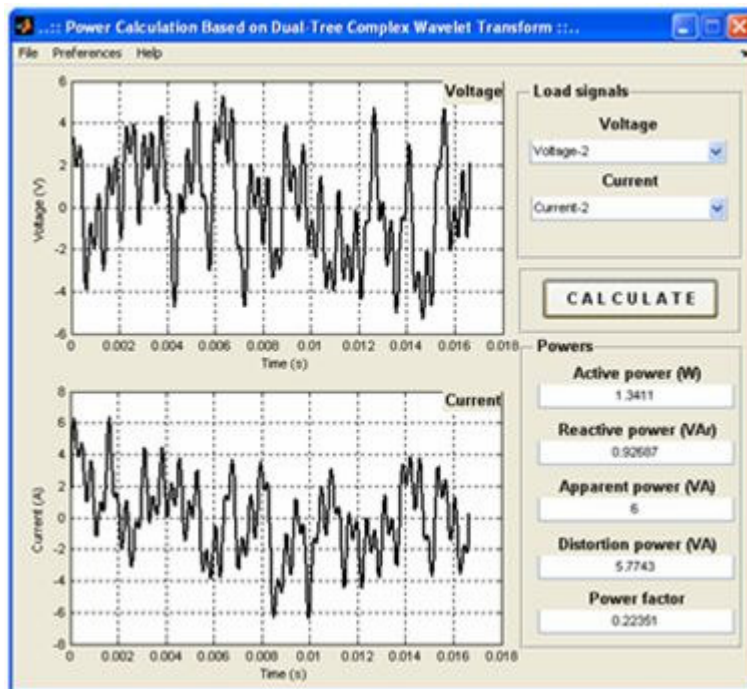


Figure 7. Screenshot for second simulation.

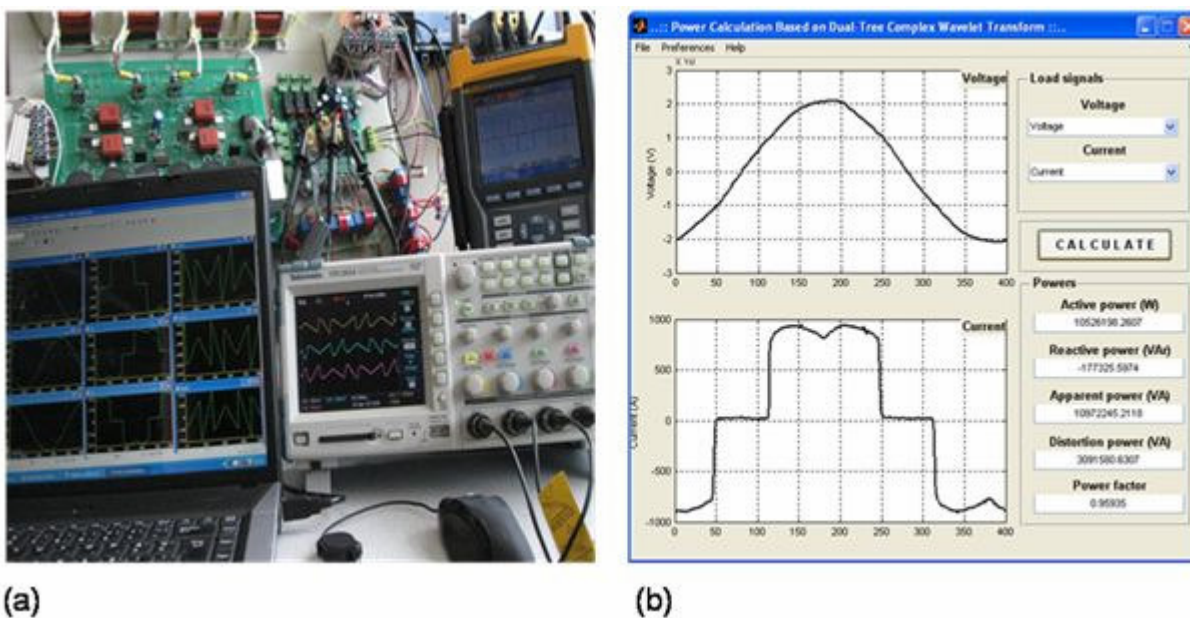


Figure 8. (a) Photo of experimental system; (b) Screenshot of graphical user interface analysis program.

DISCUSSION

In the performed work, RMS and power calculations/measurements have been made using the DT CWT. Accuracies of the proposed alternative equations have been verified using the performed comparative

simulations and the experimental measurements. In addition, it has been shown in the simulations that the DT CWT based RMS calculations are not affected from the signal shifting. As a future work, it has been intended to perform following subjects. First of all, calculation of the reactive power from the DT CWT coefficients without

using the Hilbert transform or phase shifting circuits can be made. Alternative DT CWT based approximations can be proposed for power values. Also, harmonic/interharmonic analysis can be made.

REFERENCES

- Debnath L (2002). *Wavelet Transforms and Their Applications.*, Birkhäuser, Boston.
- Goswami JC, Chan AK (1999). *Fundamentals of Wavelets.* John Wiley & Sons, USA.
- Hamid EY, Mardiana R, Kawasaki Z (2002). Method for RMS and power measurements based on the wavelet packet transform. *IEE Proc. Sci., Meas. Technol.*, 149(2): 60-66.
- IEEE Working Group on Nonsinusoidal Situations (1996). Practical definition for powers in systems with nonsinusoidal waveforms and unbalanced loads: A discussion. *IEEE Trans. Power Delivery.* 11: 79-101.
- Kingsbury N (1998). *The Dual-Tree Complex Wavelet Transform: A New Technique For Shift Invariance and Directional Filters.* IEEE Digital Signal Processing Workshop DSP. Bryce Canyon, USA.
- Morsi WG, El-Hawary ME (2009). On the Implementation of Time-Frequency Transforms for Defining Power Components in Non-sinusoidal Situations: A Survey. *Elect. Power Compon. Syst.*, 37(4): 373-392.
- Selesnick IW, Baraniuk RG, Kingsbury NG (2005). The Dual-Tree Complex Wavelet Transform. *IEEE Signal Processing Magazine.* pp. 123-151.
- The Mathworks (2000). *Wavelet Toolbox Users Guide ver. 2.* <http://taco.poly.edu/WaveletSoftware/>.
- Vatansever F, Ozdemir A (2009a). An alternative approach for calculation/measurement of fundamental powers based on wavelet packet transforms. *Sci. Res. Essays*, 4(5): 440-447.
- Vatansever F, Ozdemir A (2009b). Power parameters calculations based on wavelet packet transform. *Int. J. Elect. Power Energy Syst.*, 31: 596-603.
- Vatansever F, Ozdemir A (2010). An alternative approach for calculating/measuring fundamental powers based on wavelet packet transform and its frequency sensitivity analysis. *Elect. Eng.*, 91: 417-424.
- Yoon WK, Devaney MJ (1998). Power measurement using the wavelet transform. *IEEE Trans. Instrum. Meas.*, 47: 1205-1210.
- Yoon WK, Devaney MJ (2000). Reactive power measurement using the wavelet transform. *IEEE Trans Instrum. Meas.*, 49: 246-252.
- Zhu TX (2004). Effective value calculation in wavelet domain. *IEEE Trans. Power Delivery*, 19(1): 400-404.